Microfluidics: Mathematical Modeling and Empirical Analysis of the Burst Frequencies of a Novel Fishbone Capillary Valve and the Development of an Algorithm to Calculate its Theoretical Hold Time

Honors Thesis for Graduation with Distinction

Submitted May 2006
By Robert James Messinger

The Ohio State University
Department of Chemical and Biomolecular Engineering
Koffolt Laboratories
140 West 19th Avenue
Columbus, OH 43210

Honors Committee:

Professor L. James Lee, Advisor

Professor Shang-Tiang Yang

Approved by:

_____

Advisor

ACKNOWLEDGEMENTS

I would like to truly thank every individual that has invested his or her time in this research project. First and foremost, I would like to thank my family. Their ever-present love and support has enabled me to continually grow and achieve my potential. I would also like to wholeheartedly thank Chunmeng Lu, whose knowledge of the capillary fishbone valve and experience with the laboratory equipment were essential to the success of this project. In addition, I would like to extend a warm thank you to Dr. L. James Lee for his time, support, and general knowledge of microfluidic systems.

ABSTRACT

A highly integrated microfluidic compact-disk (CD) platform is being developed by Lee *et al* [1, 2]. The device is a polymer CD that contains fabricated arrays of microfluidic systems on its surface. This microfluidic CD platform is used in conjunction with a separate electronic unit that controls the spinning velocity of the disk and contains the appropriate biosensors for data acquisition. Centrifugal forces pump the liquid through the microchannels and passive capillary valves are used to gate fluid flow. This biomedical microdevice can be used as an integrated and portable high-throughput screening tool for enzyme linked immunosorbent assay (ELISA), clinical diagnostics, drug discovery, microreaction technology, bioseparations, etc. In order for the device to function properly, precise control of the flow sequencing must be maintained. If the working fluid is a protein or biological solution, then protein adsorption on the channel wall can change surface properties of the polymer over time. These changes in surface properties can cause the passive capillary valve to fail and disrupt proper flow sequencing within the microfluidic device. A novel "fishbone" capillary valve has been developed that seeks to overcome these problems. This valve contains a series of capillary valves arranged in the shape of a fishbone. The capillary fishbone valve must have the desired burst frequencies and a sufficient hold time in order to precisely control the flow of protein and biological fluids. In order to properly design this valve, one must have a thorough quantitative understanding of how key parameters impact the burst frequency and hold time of a fishbone. Rigorous theory and mathematical modeling have been applied to these problems to achieve this understanding. The governing equations have been derived to quantitatively calculate the burst frequencies and hold time of a capillary fishbone valve. Specifically, the general equation for the burst frequency of the *n*th fishbone within a capillary fishbone valve has been derived. Also, an algorithm has been developed to calculate the theoretical hold time of a capillary fishbone valve. Two user-friendly MATLAB computer programs have been written to calculate both the burst frequency of the *n*th fishbone and the theoretical fishbone hold time in response to key input parameters. The theory, mathematical models, algorithms, and computer programs explained in this thesis are powerful design tools for the next generation microfluidic CD platform.

TABLE OF CONTENTS

LIST OF FIGURES

LIST OF TABLES

1. INTRODUCTION

Current trends in chemistry, biology, and medicine today indicate an increased need for versatile and highly integrated high-throughput screening devices. This is particularly true for biomedical diagnostics and drug-delivery, where increased drug and health care costs have prompted the need to increase the speed and efficiency of clinical diagnostic tests and drug research and development.

The high-throughput screening devices used today in chemistry, biology, and medicine are large and very expensive automated machines that require a large sample volume and often lack complete sample processing. Usually, these machines are large robotic workstations that require a large amount of space, labor, and maintenance. Furthermore, these technologies are not portable, requiring that all tests be centralized in one location. While these technologies have greatly accelerated drug discovery and have automated chemical and biological tests for numerous applications, it is clear that there is a current need for the development of new technologies that do not possess these significant drawbacks. Given the nature of these drawbacks, it is natural to develop new high-throughput screening devices not by scaling up, but by scaling down.

Microfluidic systems hold great promise for the large-scale automation and complete integration of chemical and biological tests. Microfluidics is the study and manipulation of fluid flow through channels with at least two dimensions in the micron length scale. Devices constructed with microfluidic systems have several advantages. They are low-cost, highly portable systems that require low reagent consumption and low assay times. A wide range of microfluidic components, such as pumps, valves, mixers, and flow sensors have been demonstrated [10, 11]. Such systems have the potential for a

wide variety of applications, ranging from clinical diagnostics, bioseparations, microreaction technology, drug discovery, and on-chip flow-through PCR [1].

A microfluidic "LabCD^{TM}" has been developed for biomedical diagnostic applications and drug discovery [1, 6, 9]. The LabCD^{TM} is a polymer-based CD that contains fabricated arrays of microfluidic systems on its surface. This microfluidic platform is used in conjunction with a separate electronic unit that controls the spinning velocity of the disk and contains the appropriate biosensors for data acquisition. Centrifugal forces pump the liquid through microchannels and passive capillary valves are used to gate fluid flow. By properly designing the geometry and location of the reservoirs, microchannels, and capillary valves, one can selectively control flow sequencing within the microfluidic array by varying the centrifugal pumping force.

The LabCD^{TM} is partitioned into two separate elements. One element is the reader that contains the drive motor and biosensors for data analysis. The other element is a disposable polymer CD that contains arrays of microfluidic systems. This natural partition of functions allows the user an affordable, easy, and clean method for repeated assays.

The entire system is completely integrated. The user only needs to load the appropriate solutions to be tested (e.g., blood or urine), place the CD inside the reader, and the LabCD^{TM} performs the remainder of the work. The user can also transmit the results via the internet to a database (e.g., hospital or doctors office) for immediate medical consultation or storage in the central data bank [1]. A diagram of the LabCD^{TM} is shown below in Figure 1 [9].

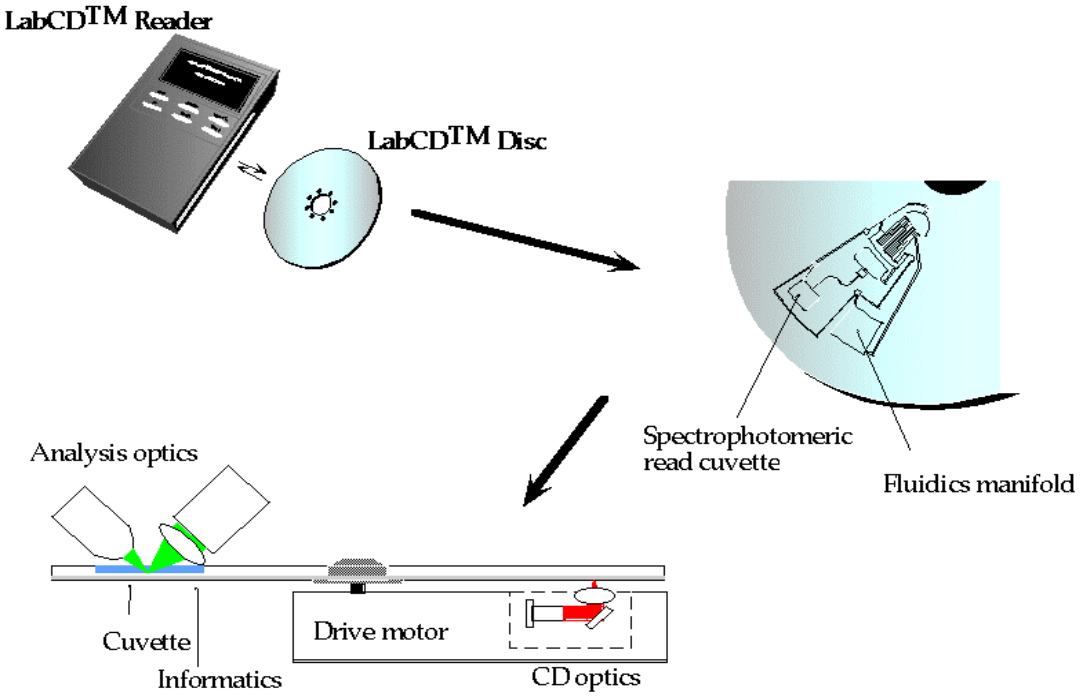

Figure 1: Partitioning of LabCD™ into Reader and Disposable Polymer CD

Note that the disposable microfluidic CD platform can be designed to perform a wide variety of functions. A polymer microfluidic CD has been developed to perform enzyme-linked immunosorbent assay (ELISA) [3]. ELISA is a widely used technique for the detection and quantification of biological agents, especially proteins and polypeptides. Today ELISA is carried out in a 96-well microtiter plate in a tedious and labor intensive process. Assay time typically ranges from many hours to up to 2 days. The CD ELISA has been tested to be a completely integrated system allowing an overall assay time of about one hour for ELISA with rat IgC from hybridoma cell culture [3]. This assay time is dramatically shorter than the typical microtiter ELISA process while using fewer reagents and retaining the same detection range as the conventional method.

Figure 2 illustrates the design of the microfluidic ELISA CD [3]. The substrate, conjugate, washing solution, primary antibody, blocking protein, and antigen solution are preloaded into the corresponding reservoirs before the test. The flow sequence can be designed such that the first antibody is initially released at a low rotation speed. After incubation and antibody adsorption on the microchannel surface, the CD is spun at a higher rate to release the washing solution that removes all unbounded antigens. The blocking solution is then released to bind with unbounded surface sites on the channel wall. After incubating and washing, the antigen is released to complex with the antibody. After another period of incubating and washing, the conjugate, or second antibody, is released to complex with the antigen; this binding effectively "sandwiches" the antigen between the antibodies. Finally, after the last stage of incubation and washing, the substrate is released and reacts with the conjugate to produce a measurable signal. This signal is usually colorimetric or fluorescent.

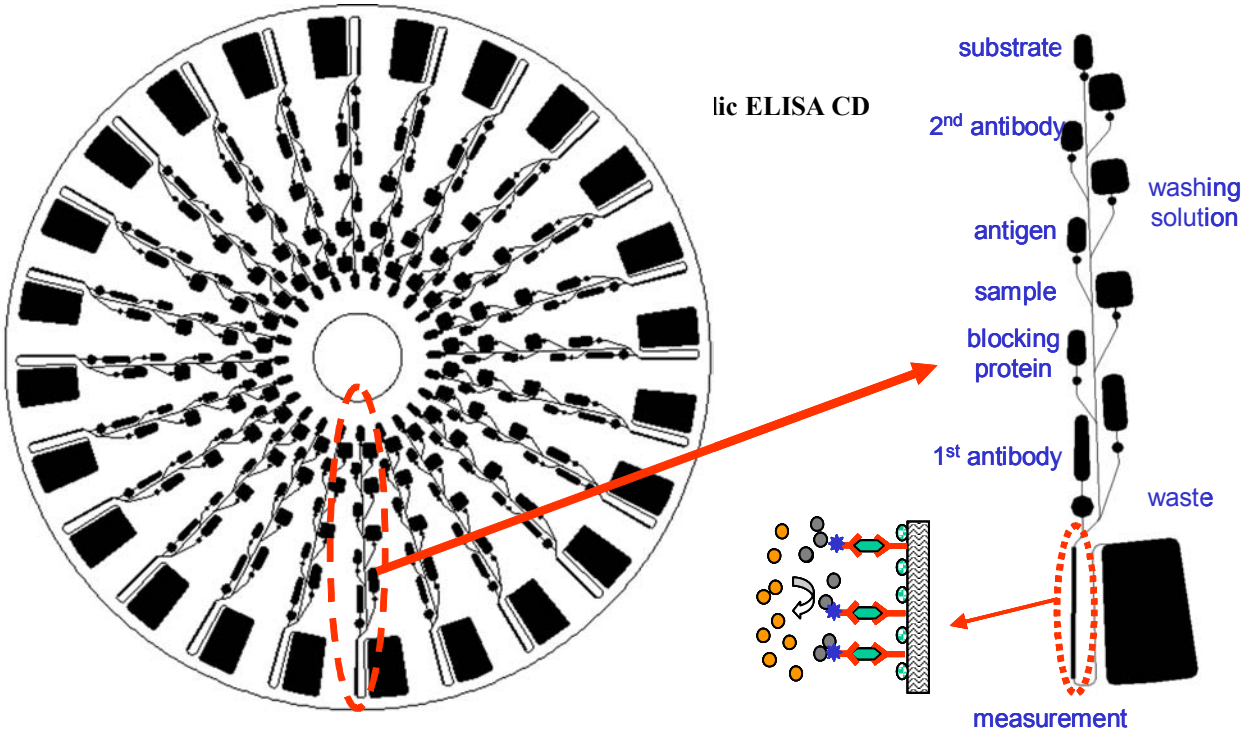

However, protein adsorption on the microchannel wall can cause the surface properties to change over time. Since the presence of the bound protein will cause the polymer wall to become increasingly hydrophilic, the contact angle between the solid polymer and the liquid solution will decrease over time. Because the protein adsorption will eventually reach equilibrium, the resulting contact angle will naturally begin at an initial angle and monotonically decrease to a final equilibrium contact angle.

This kinetic increase of the hydrophilicity of the polymer has an effect on the performance of the capillary valve. As a liquid flows through a sudden expansion, asymmetric intermolecular forces at the liquid-air interface generate an opposing surface tension force. If the net capillary pressure due to the surface tension force is greater than the net centrifugal pumping pressure, the capillary valve will hold the liquid. However, the magnitude of the surface tension force, and hence the opposing capillary pressure, is very sensitive to the magnitude of the contact angle. Thus, a capillary valve that initially holds a flowing fluid could fail over time as protein adsorption renders the surface increasingly hydrophilic, decreasing the contact angle and hence the opposing capillary pressure.

A novel "fishbone" capillary valve has been developed that seeks to overcome these problems. This valve contains a series of capillary valves arranged in the shape of a "fishbone." If the first fishbone (capillary valve) fails within the entire fishbone valve due to protein adsorption, the fluid will flow to the second fishbone, and then to the third, etc. These capillary valves provide the necessary redundancies to hold the fluid for a prolonged period of time when protein adsorption causes premature valve failure. A picture of the capillary fishbone valve is shown in Figure 3. The channel width is 100μm.

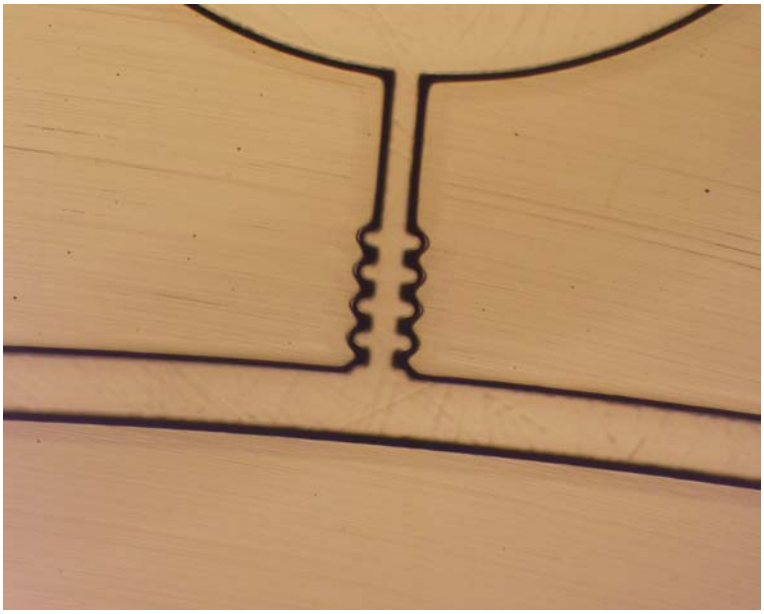

Figure 3: Capillary Fishbone Valve

A picture of the capillary fishbone valve halting fluid flow is shown below in Figure 4. The channel width is 100μm. Note that the first fishbone eventually failed due to protein adsorption but the resulting flow was temporarily halted by the second fishbone. After the second fishbone fails, the third fishbone held the flow, etc.

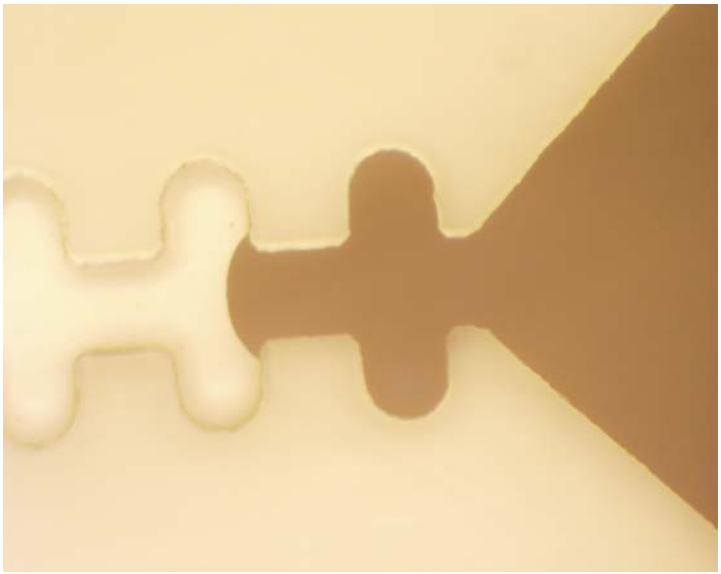

Figure 4: Capillary Fishbone Valve Halting Fluid Flow

The capillary fishbone valve must have the desired burst frequencies and a sufficient hold time in order to precisely control the flow sequencing within the microfluidic system. However, in order to do so, one must have a thorough quantitative understanding of how key parameters impact the burst frequencies and hold time of a capillary fishbone valve. The fluid properties, the spin frequency of the microfluidic CD, and the geometry and location of the microchannels, reservoirs, and capillary fishbone valve will all affect the magnitude of the burst frequency.

In this thesis, rigorous theory and mathematical modeling have been applied to produce a quantitative understanding of how these key parameters affect the burst frequencies and hold time of a capillary fishbone valve. The resulting theory, models, algorithms, and MATLAB computer programs are powerful design tools for the general microfluidic CD platform discussed above, including the ELISA CD.

2. LITERATURE REVIEW

The fundamental fluid physics changes dramatically when the length scale is decreased to the micron level. For example, mass transport in microfluidic devices is generally dominated by viscous dissipation, and inertial effects are generally negligible [10]. Diffusion lengths are often small and the surface to volume to ratio is higher than in macroscopic systems. These can both lead to increased reaction efficiency and lower assay times as demonstrated by the microfluidic ELISA CD [3]. Fluid-surface interactions often become dominate in microfluidic systems. These interactions are important because asymmetric intermolecular forces at fluid interfaces can give rise to significant surface tension effects when the fluid is in a channel in the micron length scale. It has been shown that fluid flow in a microchannel can be stopped by introducing a sudden expansion, which generates an opposing capillary pressure due to surface tension [5]; this phenomena is the concept behind the capillary valve. In addition, fluid flow through the microchannels is usually laminar since the Reynolds number (ratio of inertial forces/viscous forces) is usually very small. With water as the working fluid, typical velocities of 1 μm/s – 1 cm/s, and typical channel radii of 1-100 μm, the Reynolds number ranges between 10^{-6} and 10 [10].

There are several existing techniques for the control and manipulation of fluid flow in microchannels. In general, flow can be driven electrically, thermally, or mechanically.

Electrokinetically driven flows are the most popular and well-developed group of methods for pumping and driving fluid flow in the microfluidics field. Electroosmosis, electrohydrodynamics, and electrowetting are common electrokinetic manipulation

techniques [1]. Electrokinetic flow has many advantages: it is easy to control the fluid using a computer-controlled voltage and a series of electrodes, it can often be used for electrochemical separations based off of size and charge differences, and it can easily be implemented in a wide number of materials (glass, quartz, polymers, etc.) using microfabrication techniques [6]. Electrokinetically driven flow also scales favorably towards miniaturization. However, it also has many disadvantages. Electrokinetic flow depends strongly upon the physiochemical properties of the fluid, particularly the pH and the ionic strength; this often makes it difficult to pump biological fluids such as blood or urine. Also, electrokinetic flow requires that the fluid be in a continuous state such that no air bubbles are present in the microchannels that break up the continuity of the fluid [10]. A large voltage is often required, reducing portability. Another issue with electrokinetic flow is that it can produce unwanted Faradaic reactions.

Controlling fluid flow via thermal gradients is another developing microfluidic technique. In this method, a surface is embedded with microheaters that can be selectively activated to establish local thermal gradients within a fluid droplet [12]. This thermal gradient gives rise to interfacial surface tension gradients. Since a droplet will move in a manner to lower its total associated interfacial energy, these thermal gradients will ultimately drive fluid flow. However, this technology can be difficult and expensive to implement and requires very precise control of the local fluid temperature.

Fluid flows can also be manipulated mechanically. Mechanical manipulation of the flow is a robust method for pumping fluids, particularly biological fluids, because the methods are insensitive to certain physiochemical fluid properties such as pH and ionic strength. A blister pouch design [9] and an acoustic pump [11] are two pressure based

methods of driving fluid flow. However, the blister pouch does not miniaturize well and the acoustic pump is expensive and limits the choice of materials to piezoelectrics.

The microfluidic CD device studied in this thesis uses a centrifugal pumping force to drive fluid motion through a microchannel. In centrifugal pumping, fluid flow is driven via rotationally induced hydrostatic pressure. This mechanical pumping method is low cost, insensitive to fluid pH and ionic strength, is capable of fine flow control, and is easily integrated with information carrying capacity of the CD [1].

One of the essential components of any microfluidic system is the ability to start and stop flow. This control over the flow of liquid is usually performed with valving mechanisms. Valving mechanisms can be divided into two general categories: active valves and passive valves.

Some examples of active valves include a pneumatically-controlled membrane [15], surface wetting [16], an electrochemically-controlled bubble [17], and thermally activated gels [18]. Active valves usually require an external stimuli or a moving part that is often difficult to scale down as the device becomes increasingly miniaturized. Passive valves include a hydrophobic valve [4], polymer check valve [13], elastomer valve [14], and capillary valve [9]. Passive valves provide a very flexible method for increased miniaturization of microfluidic systems. Furthermore, passive valves tend to be more cost effective than active valves.

The microfluidic CD device described in this thesis uses a variation of the capillary valve known as the fishbone capillary valve. This valve and its applications are described in the Introduction. Until now, theory and mathematical modeling have not been applied to quantitatively understand the performance of the capillary fishbone valve.

3. EXPERIMENTAL METHODS

3.1 Making the PDMS Microfluidic Mold

The PDMS daughter mold was obtained by thoroughly mixing a 10:1 (w/w) base/curing agent of poly(dimethylsiloxane) (PDMS) and then degassing the mixture under vacuum for 30 minutes. It was then poured over a SU8/silicon mother mold and cured on a hot plate at 70 °C for 2 hours. The SU8/Silicon mother mold was previously fabricated with the photolithographic process [2]. The PDMS daughter mold was used to produce poly(methyl methacrylate) PMMA microfluidic systems with capillary valves through the microembossing process.

3.2 Making the PMMA Microfluidic System

The PMMA microfluidic systems were created using the PDMS daughter molds and a microembossing process. PMMA pellets were stored under vacuum and inside an isothermal environment at 70 °C; these conditions allowed the PMMA pellets to remain dry and below its glass transition temperature of 105 °C. These pellets were placed on the PDMS daughter mold, which in turn was placed between two glass plates. The PMMA, PDMS, and glass plates were placed on a Carver two-post manual hydraulic press. The surface of the hydraulic press was previously elevated to 180 °C with the external temperature regulator. The hydraulic press was compressed until resistance was achieved and the system was allowed to thermally equilibrate for 15 minutes. After thermal equilibration, the melted PMMA can be compressed further and forced into the PMMA daughter mold. After allowing the system to set for 15 minutes, the mold was removed and allowed to cool to room temperature. The glass plates and PDMS daughter

mold were separated from the PMMA microfluidic system. A picture of a PMMA microfluidic CD is shown below in Figure 5.

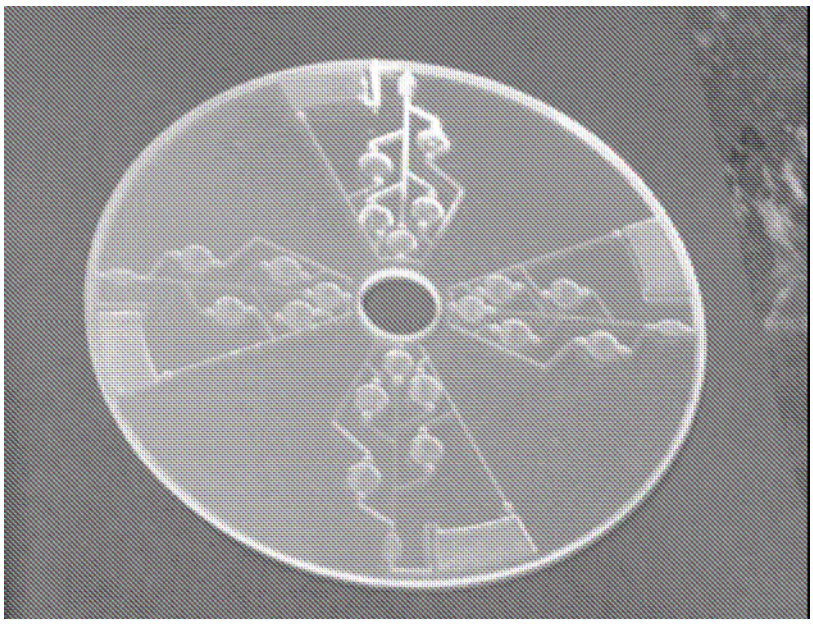

Figure 5: PMMA Microfluidic System

3.3 Plasma Treatment of PMMA

The PMMA was plasma treated to increase its hydrophobicity. Specifically, the PMMA was coated with a molecular layer of carbon hydrotriflouride (CHF_3). The Micro-RIE (Technics 800II RIE System) was used for the plasma treatment. The power, gas flow rate, and treatment time are 300 wattts, 50 sccm, and 2 minutes, respectively.

3.4 Kinetic Contact Angle Measurements in Sealed Chamber

In order to predict the burst frequency of a fluid in a microchannel, the contact angle between the fluid and the solid must be known accurately. Since protein adsorption on the PMMA surface renders the polymer surface increasingly hydrophilic, the contact angel as a function of time must also be measured. In particular, the initial and equilibrium contact angles are important to the net hold time of the capillary fishbone

valve. A device was constructed to measure the kinetic contact angle between a fluid and a solid; a schematic of this device is included in Figure 6.

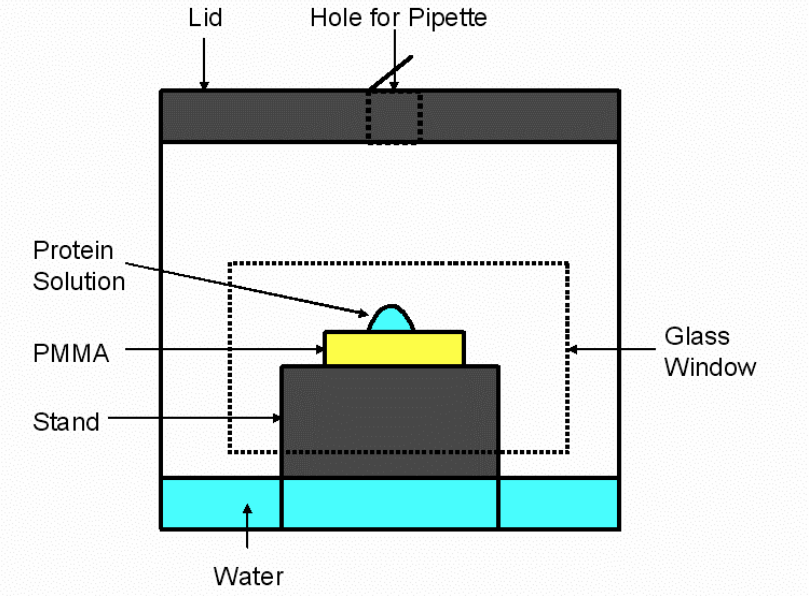

Figure 6: Sealed Chamber for Measurement of Kinetic Contact Angles

The PMMA chips were cleaned with distilled water, soaked in a 1.0 wt% BSA (Bovine Serum Albumin) protein solution for 10 minutes, and then dried with a nitrogen hose. The BSA protein treatment simulates the protein blocking step that occurs in the ELISA process.

A chip of PMMA was placed on a stand, which in turn was placed in a plastic jar. The jar was partially filled with water to establish a water vapor-liquid equilibrium to prevent evaporation during testing. A small hole was cut from the lid of the jar and covered with Scotch tape. A square section was cut out of the plastic jar and replaced with glass to ensure the microscope could view the PMMA surface and droplet. After the stand and PMMA chip was placed in the jar and the jar was partially filled with water, the environment was allowed to equilibrate for five minutes. Then, the Scotch tape on

the top of the lid was removed, the pipette was inserted, and a drop of 0.2 wt% BSA protein solution was added to the PMMA drop. The pipette was removed and the Scotch tape was placed back to seal the chamber. A microscope was connected to a VCR and a computer; a digital picture of the contact angle of the droplet was taken every minute over the course of five minutes.

Using a MATLAB program, a discretized X-Y coordinate system was manually assigned along the interface of the sessile droplet. A polynomial was fit to each side of the droplet and the first derivative of the polymer was computed. This derivative was evaluated at the point where the three phases (solid-liquid-air) meet to calculate the slope of the tangent line at this point. The angle from the solid, through the liquid, and to the tangent line determines the contact angle of the droplet. The left and right contact angles of the droplet, although very similar, were averaged.

3.5. Burst Frequency Measurements of Capillary Fishbone Valve

The PMMA chips were cleaned with distilled water, soaked in a 1.0 wt% BSA (Bovine Serum Albumin) protein solution for 10 minutes, and then dried with a nitrogen hose. Again, the BSA protein treatment simulates the protein blocking step that occurs in the ELISA process. The channels were closed with industrial Scotch tape that acts as the top channel surface.

After cleaning and protein treatment, each chip was taped on a CD for mechanical support. The loading reservoir was loaded with a 0.2 wt% BSA solution that was previously dyed green. The system was allowed to equilibrate for 5 minutes. This CD was placed on the a motor plate designed by Gamera Bioscience, which was connected to an encoder to trigger the strobe (Monarch, DA 115/Nova Strobe) for synchronized

imaging. When the same position of the CD passed under a CCD camera (Panasonic GP-KP222), the strobe is triggered. Since the CD spins at the same rate at which the strobe light is triggered, a fixed position of the CD is highlighted in each turn. The image of the CD can be captured via the CCD camera and then sent to a computer for data storage. A schematic of this setup is shown in Figure 7. A picture of the actual experimental setup for the burst frequency measurements is shown in Figure 8.

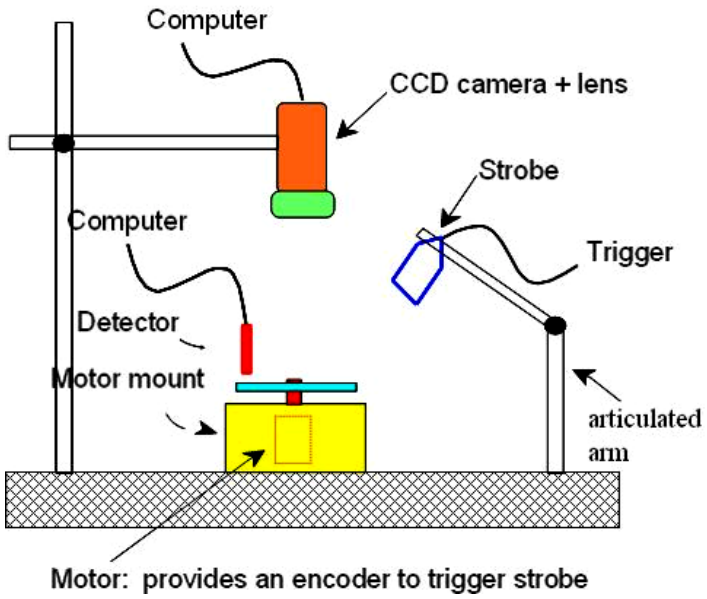

Figure 7: Schematic of Experimental Setup for Burst Frequency Measurements

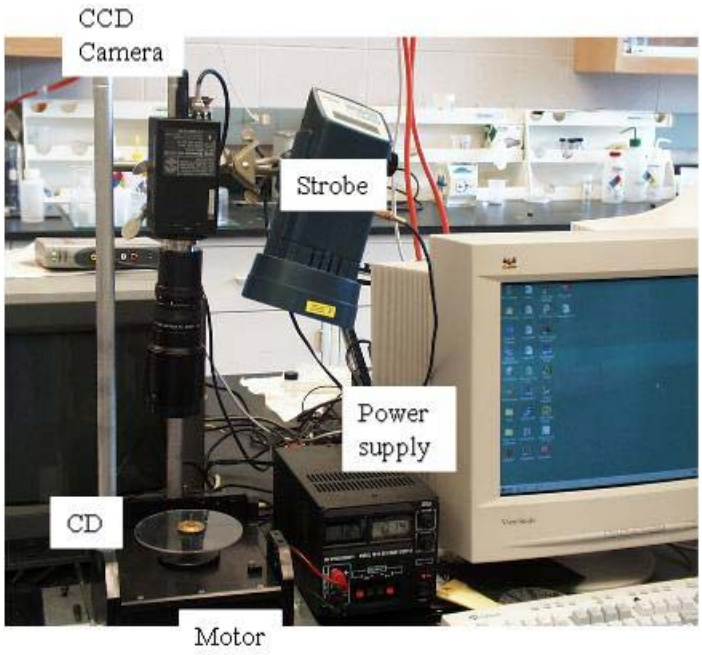

Figure 8: Actual Experimental Setup for Burst Frequency Measurements

It should be noted that the RPM of the CD increases by about 30 RPM's each time the spinning program's input is increased by an incremental value of one. Thus, any empirical measurement actually yields a burst frequency range; the actual burst frequency of the valve lies somewhere between the lower and upper bound of the burst frequency range. Also, it should be noted that all empirical burst frequency measurements were carried out in the clean room.

4. THEORY AND DERIVATIONS

4.1 Definition of Variables

Table 1 summarizes the definition of each variable that will be used in the derivations.

Table 1: Definition of Variables

Variable	Definition
wc	Width of microchannel
hc	Depth of microchannel
wf	Width of fishbone valve
d	Distance between fishbones within a fishbone valve
n	Number of fishbones within a fishbone valve
R_1	Distance from CD center to beginning of fluid reservoir
R_2	Distance from CD center to end of fluid flow front
ρ	Fluid density
γ	Air-liquid surface tension
θ	Top-view contact angle (width direction)
Φbot	Side-view contact angle on top of channel (height direction)
Φtop	Side-view contact angle on bottom of channel (height direction)
f	Actual spin frequency of the CD
fbn	Burst frequency of *n*th fishbone in fishbone valve
t_j	Discretized time value at time t_j
Fh,top	Surface tension force vector on top of channel from side-view (height direction)
Fx,h,top	X-direction surface tension force vector on top of channel from side-view (height direction)
Fh,bot	Surface tension force vector on bottom of channel from side-view (height direction)
Fx,h,bot	X-direction surface tension force vector on bottom of channel from side-view (height direction)
Fw	Surface tension force vector on one wall from top-view (width direction)
Fx,w	X-direction surface tension vector on one wall from top-view (width direction)
Net Hold Time	Net hold time of a capillary fishbone valve
i	Denotes row element *i* in matrix (*i,j*)
j	Denotes column element *j* in matrix (*i,j*)

In the derivations, three diagrams are provided to further illustrate the definition of these variables. A top view diagram of a liquid in a capillary fishbone valve, a side

view diagram of a liquid in a capillary fishbone valve, and a top view diagram of an entire capillary fishbone valve will be shown.

4.2 Derivation of *ΔPs*, Capillary Pressure

A top view diagram of a liquid halted in a fishbone valve due to an opposing capillary pressure is shown in Figure 9.

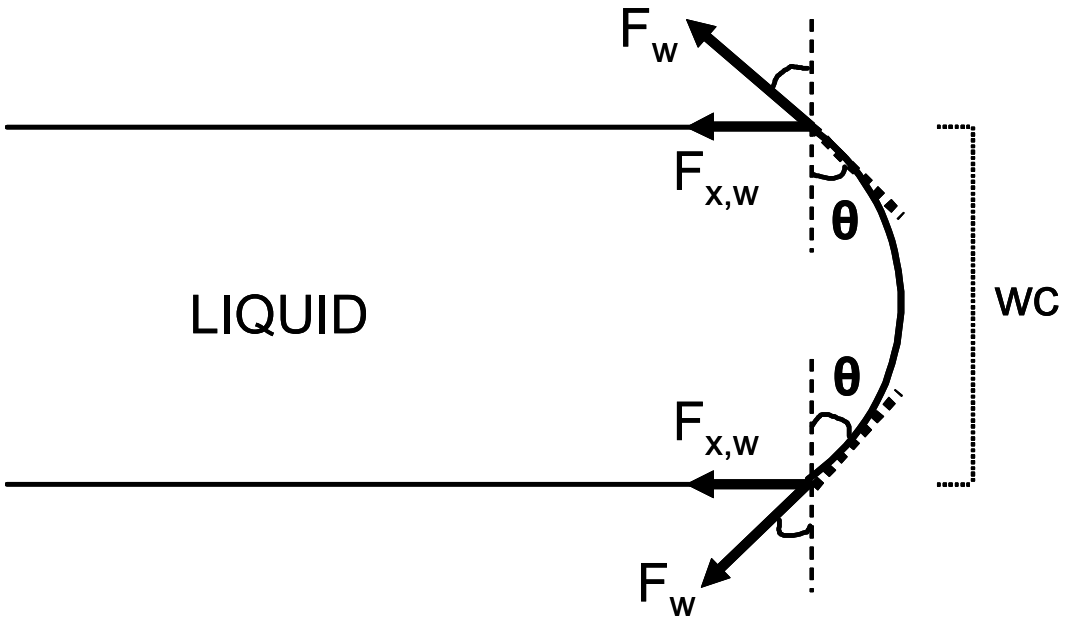

Figure 9: Top View of Liquid in Capillary Fishbone Valve

When a liquid flowing through a microchannel reaches a sudden expansion, asymmetric intermolecular forces at the interface generate surface tension forces that oppose the flow. From the top view of the fishbone valve (width direction), a fluid will make a contact angle θ with the side walls of the channel. Since both of the side walls in the microfluidic CD are made out of the same polymer (PMMA), these two angles are identical. The surface tension force vector on one wall is *Fw* (surface tension force from width view), and its x-direction vector component is *Fx,w*.

The contact line for each wall is *hc*, the height of the channel. If the opposing surface tension force is assumed to be equal in magnitude along the height of the channel, then a mechanical force balance yields:

$$F_{x,w} = (\gamma * hc) * \sin(\theta) \quad (1)$$

It should be noted that the walls beyond the expansion in the width direction are not wetted. Thus, if the fluid is a protein solution or biological fluid, the top view contact angle θ will not decrease with time due to protein adsorption on the surface.

A side view diagram of a liquid in a capillary fishbone valve is shown in Figure 10.

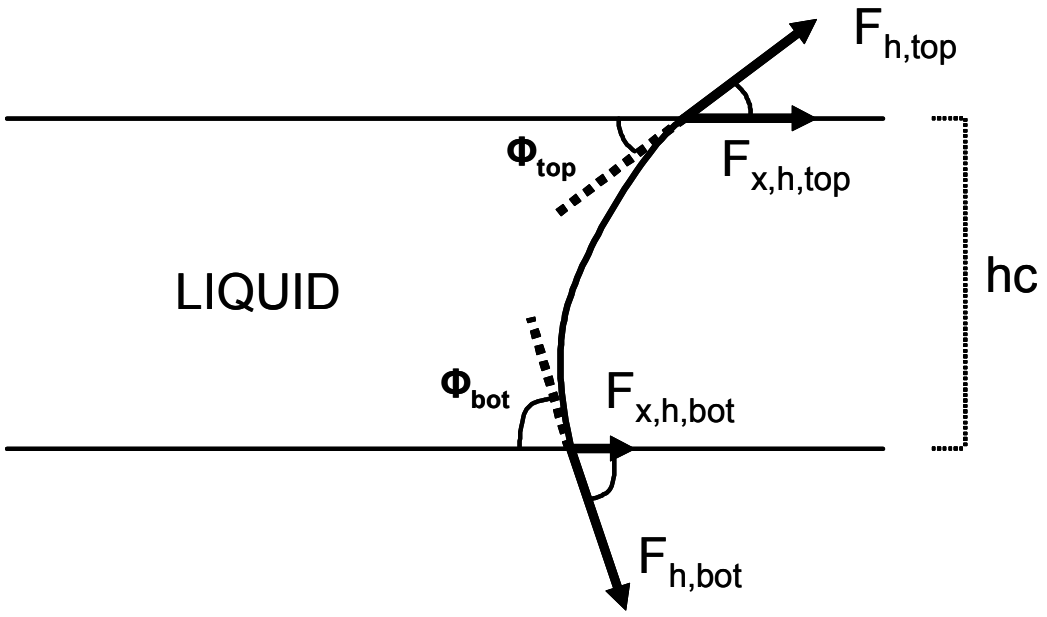

Figure 10: Side View of Liquid in Capillary Fishbone Valve

In the microfluidic CD platform under analysis, the height of the microchannels is constant throughout the entire microfluidic system. While a fluid flowing into a capillary fishbone valve experiences a sudden expansion in the width direction (top view), it does not experience a sudden expansion in the height direction (side view). Thus, surface tension forces will promote flow in this direction rather than oppose flow. Also, the top material (industrial Scotch tape) and the bottom material (PMMA) are different; this gives rise to a different contact angle on the top of the channel (Φtop) than the contact angle on the bottom of the channel (Φbot). The surface tension force vector on the top of the channel is channel is *Fh,top* (surface tension from height direction on top of channel) and its x-direction component *Fx,h,top*. Likewise, the surface tension force vector on the bottom of the channel is *Fh,bot* and its x-direction component is *Fx,h,bot*.

In this case, the contact line for both the top and bottom walls is *wc*, the width of the channel. If the surface tension force is assumed to be constant along the width of the channel, then a mechanical force balance on the top wall yields:

$$F_{x,h,top} = (\gamma * wc) * \cos(\Phi_{top}) \quad (2)$$

A mechanical force balance on the bottom wall yields:

$$F_{x,h,bot} = (\gamma * wc) * \cos(\Phi_{bot}) \quad (3)$$

It should be noted that the walls of the channel are wetted by the fluid. If the fluid is a protein solution or biological fluid, both of the contact angles *Φtop* and *Φbot* will monotonically decrease over time to a new equilibrium value. This kinetic decrease in contact angle occurs due to protein adsorption on the surface of the channel; this protein adsorption renders the polymer more hydrophilic. This phenomenon significantly affects the calculation of the theoretical fishbone hold time, which will be discussed in detail later (section 5.2).

The resulting capillary pressure generated from the expansion can be calculated by dividing the net surface tension force acting on the fluid by the channel area.

$$\Delta P_S = \left[\frac{2 * F_{x,w}}{A} - \frac{F_{x,h,top}}{A} - \frac{F_{x,h,bot}}{A} \right] \tag{4}$$

Again, note that the surface tension forces from the top view oppose flow and the side view surface tension forces promote flow. The area is simply the product of the width and height of the channel. Thus, substituting equations (1), (2), and (3) into equation (4) yields the net capillary pressure due to surface tension:

$$\Delta P_S = \left[\frac{2 * \sin(\theta)}{wc} - \frac{\cos(\Phi_{top})}{hc} - \frac{\cos(\Phi_{bot})}{hc} \right] \tag{5}$$

A more thorough derivation that includes intermediate steps and calculation is included in Appendix 1.

4.3 Derivation of *fb*, the Burst Frequency of a Capillary Fishbone Valve

The burst frequency of a capillary valve is defined as the spinning frequency of the CD for which the capillary valve will fail. The valve will fail when the centrifugal pumping pressure exceeds the net capillary pressure due to surface tension.

The derivative of the centrifugal pumping pressure with respect to radial CD position is:

$$\frac{dP_c}{dr} = \rho * \omega^2 * r \tag{6}$$

This differential equation can be integrated from radius R_1 to R_2 to yield the final expression of the centrifugal pumping pressure:

$$\Delta P_c = \rho * \omega^2 * \Delta R * \overline{R} \tag{7}$$

Where ΔR is equal to $(R2 - R1)$ and $\overline{R}$ is equal to $(R1 + R2)/2$. To solve for the burst frequency, the net capillary pressure due to surface tension that opposes flow (equation 5) is set equal to the centrifugal pumping pressure (equation 7). This relationship yields the final expression for the burst frequency:

$$fb = \sqrt{\left(\frac{\gamma}{4\pi^2 \rho \Delta R \overline{R}}\right)\left(\frac{2*\sin(\theta)}{wc} - \frac{\cos(\Phi_{top})}{hc} - \frac{\cos(\Phi_{bot})}{hc}\right)} \tag{8}$$

A more thorough derivation that includes intermediate steps and calculation is included in Appendix 2.

4.4 Derivation of *fbn*, the Burst Frequency of the *n*th Fishbone

A capillary fishbone valve contains a number of "fishbones" that act as separate and redundant capillary valves. Each fishbone within a fishbone valve has a unique burst frequency; the burst frequency of the 1st fishbone will naturally be higher than the burst frequency of the 2nd fishbone since the centrifugal pumping pressure increases as the distance from the center of the CD to the flow front (R_2) increases. Likewise, the burst frequency of the 2nd fishbone will be greater than that of the 3rd fishbone, and so on.

Each fishbone within a fishbone valve is a fixed distance from the last. Specifically, this distance is the sum of the width of one fishbone (*wf*) plus the distance between fishbones (*d*). A top view diagram of an entire capillary fishbone valve is shown below in Figure 11. The fishbones are numbered from 1 to *n*. The width of the channel (*wc*), the width of the fishbone (*wf*), and the distance between fishbones (*d*) are labeled.

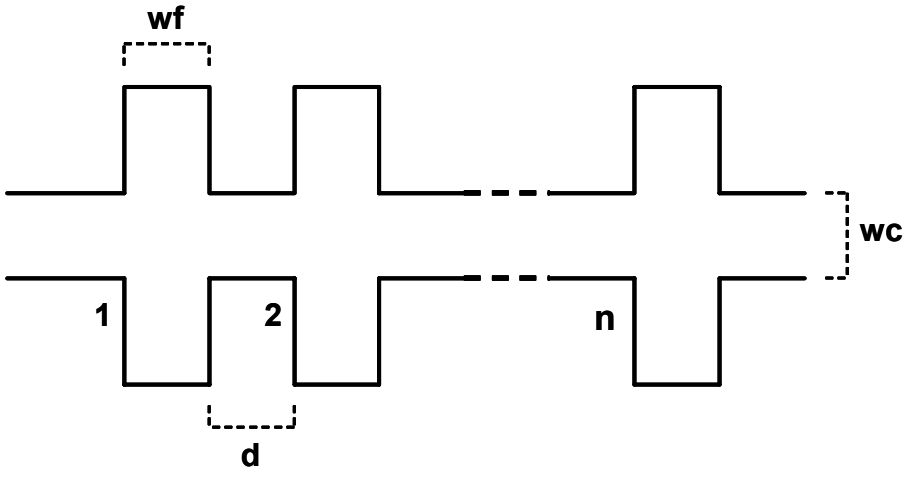

Figure 11: Top View Diagram of Entire Capillary Fishbone Valve

To generalize the burst frequency to equal the burst frequency of the *n*th fishbone, the distance from the center of the CD to the end of the fluid flow front (R_2) must be increased by a factor of (n-1)(wf +d). This generalized equation yields the following general relationship:

$$fbn = \sqrt{\left(\frac{\gamma}{4\pi^2 \rho \left[R_2 - R_1 + (n-1)(d+wf) \right] \left[\frac{R_1 + R_2 + (n-1)(d+wf)}{2} \right]} \right) \left(\frac{2 * \sin(\theta)}{wc} - \frac{\cos(\Phi_{top})}{hc} - \frac{\cos(\Phi_{bot})}{hc} \right)} \quad (9)$$

The burst frequency of the *n*th fishbone is a function of twelve parameters: the air/liquid surface tension, the contact angles of the liquid from the top view, the top contact angle of the liquid from the side view, the bottom contact angle of the liquid from the side view, the density of the fluid, the distance between the center of the CD and the beginning of the fluid in the reservoir, the distance between the center of the CD and the end of the fluid flow front, the width of the channel, the height of the channel, the width of a fishbone, the distance between fishbones, and the number of the fishbone within the fishbone valve. Mathematically, this can be concisely represented:

$$fbn = f(\gamma, \theta, \Phi_{top}, \Phi_{bot}, \rho, R_1, R_2, wc, hc, wf, d, n) \quad (10)$$

If the working fluid is a biological fluid or protein solution, then protein adsorption on the channel wall will render the polymer more hydrophilic, decreasing the side view contact angles and over time. In this case, the burst frequency is also a function of time. A kinetic model for both $\Phi tot(t)$ and $\Phi bot(t)$ must be known in order to

calculate the burst frequencies as a function of time. These kinetic models are also necessary to understand how the disparity between the initial and equilibrium contact angle will affect the performance of the capillary fishbone valve. This information combined with equation 9, can be used to calculate the theoretical hold time of a specified capillary fishbone valve. The algorithm for this calculation is discussed in section 5.2.

A more thorough derivation that includes intermediate steps and calculation is included in Appendix 3.

5. MATLAB COMPUTER PROGRAMS & ALGORITHMS

5.1 Array of Burst Frequencies for *n* Fishbones within a Capillary Fishbone Valve

A MATLAB program has been written that calculates an array of burst frequencies for *n* fishbones within a capillary fishbone valve.

The program takes 12 input parameters. The user specifies the channel and fishbone geometries (*wc*, *hc*, *wf*, *d*, *n*), fishbone valve location (R_1 and R_2), fluid properties (ρ, γ), and the top and side view contact angles (θ, Φbot, Φtop).

Algorithmically, this program uses a loop to calculate the burst frequency of each individual fishbone within the fishbone valve. The loop performs a number of iterations equal to the number of *n* fishbones within the fishbone valve; thus, the resulting array will have a number of elements equal to *n*. Element 1 corresponds to the burst frequency of the 1st fishbone, element 2 corresponds to the burst frequency of the 2nd fishbone, etc. Equation 9 is used to calculate the burst frequency of each individual fishbone during each iteration of the loop.

The MATLAB program code is included in Appendix 4. A sample output to this program is included in Appendix 5.

This program assumes that all parameters are independent of time. This assumption is valid when the working fluid does not alter the surface properties of the polymer over the time. For the calculation of kinetic burst frequencies and the net hold time of the fishbone valve, please see the next MATLAB program and its corresponding algorithm (section 5.2).

5.2 Theoretical Capillary Fishbone Valve Hold Time: Algorithm and Program

A MATLAB program has been written that calculates the theoretical hold time of a fishbone valve under user specified conditions.

The program takes 11 input parameters and 2 input functions. The user specifies the channel and fishbone geometries (*wc*, *hc*, *wf*, *d*, *n*), fishbone valve location (*R1, R2*), fluid properties (ρ, γ), the top view contact angle (θ), kinetic models for the side view contact angles as a function of time ($\Phi bot(t)$ and $\Phi top(t)$), and the actual spin frequency of the disk (*f*). The kinetic models are discretized into a number of elements equal to the number of *j* elements of the defined time vector *t*.

There are three general cases that occur when calculating the hold time of a fishbone. In the first case, the actual spin frequency of the disk exceeds the burst frequency of each fishbone within the fishbone valve over the entire time domain. In this case, the fluid will simply burst through each individual fishbone in the fishbone valve such that the hold time of the capillary fishbone valve is zero. In the second case, the actual spin frequency of the disk is below the burst frequency of each fishbone in the fishbone valve over the entire time domain. The hold time of the capillary fishbone valve in this case will be infinite; the valve will hold indefinitely until the CD is accelerated to a sufficient RPM where the centrifugal pumping pressure exceeds the net capillary pressure due to surface tension. The third case occurs when the actual spin frequency of the disk is less than the burst frequency of the first fishbone at time zero, but the burst frequency of the fishbone falls below the actual spin frequency of the disk at some time t_j due to protein adsorption. The redundancies within the capillary fishbone valve are specifically designed for this case. The overall hold time of a capillary fishbone valve is simply the sum of the individual hold times of each fishbone within the valve.

The three general cases can be summarized as follows:

i. Case #1:

$f > fbn$ for all t_j and for all n

Net Hold Time = 0

ii. Case #2:

$f < fbn$ for all t_j and for all n

Net Hold Time = ∞

iii. Case #3:

$f < fb1$ at $t = 0$ for first fishbone

$f > fb1$ for $t = t_j$ for first fishbone

$(Hold\ Time)_{\text{ith fishbone}} = t_j$ for which $f > fbi$

$Net\ Hold\ Time = \sum(Hold\ Time)_{\text{ith fishbone}}$

A MATLAB program was written to calculate the net theoretical hold time of a capillary fishbone valve. First, the MATLAB program calculates a matrix of burst frequencies. Each row corresponds to the *n*th fishbone within the fishbone valve and each column corresponds to a discretized time value (t_j) as specified by the kinetic model for the side view contact angles. Thus, matrix element (i,j) represents the burst frequency of the i^{th} fishbone at discretized time value t_j. Each row can be thought of as a "kinetic burst frequency" for the i^{th} fishbone. The program uses equation 9 to calculate the burst

frequencies. The program also asks the user if he or she wishes to display this burst frequency matrix for reference as part of the program output.

After the matrix of burst frequencies has been calculated, the actual spin frequency of the disk is systematically compared with each value in this matrix to determine the overall hold time of the capillary fishbone valve. Algorithmically, the program uses a nested loop to compare these values. The outer loop performs a number of iterations equal to the number of n fishbones present in the fishbone valve; this number is equal to i number of rows in the burst frequency matrix. The inner loop performs a number of iterations equal to the number of values of discretized time t_j as specified by the kinetic contact angle model; this number is equal to j number of columns in the burst frequency matrix.

The outer loop begins with the first fishbone (row $i = 0$) and then moves sequentially to the nth fishbone (row $i = n - 1$). When the program checks the first fishbone, it compares the actual spin frequency of the disk with the calculated burst frequency of the fishbone at time value $t = 0$. If the actual spin frequency is greater than the burst frequency, then the valve will fail. If the valve fails, it assigns a value of "false" to a defined logic operator and assigns a hold time value for this fishbone as equal to the current time element t_j (in the case of immediate valve failure, the hold time for the first fishbone is zero). The program then breaks from the inner time loop to start a burst frequency comparison of the next fishbone in the outer loop. However, if the actual spin frequency is less than the burst frequency of the first fishbone, then the valve will hold. In this case, the program will assign a value of "true" to a defined logic operator and it will move in the inner loop to the next burst frequency associated with the next time

element $t = t_j$. Using the same algorithm, it will then compare the actual spin frequency of the disk with the burst frequency of the fishbone evaluated at this time. If the actual spin frequency exceeds the burst frequency at $t = t_j$, the hold time = t_j for this fishbone and the logic operator is assigned a value of "false." If the actual spin frequency is less than or equal to the burst frequency, then the valve holds, the logic operator is assigned a value of "true," and the program moves on to the next fishbone burst frequency associated with the next time value t_j.

If the first fishbone valve within the fishbone does not fail over the entire time domain (i.e. the initial and equilibrium contact angles are sufficient to halt the fluid flow), then the entire capillary valve will hold the fluid and the capillary fishbone valve hold time is infinite at these conditions. This occurrence is identical to "Case 2." In this case, the program will have assigned a final value of "true" for the defined logic operator. If this logic operator has a value of true after execution of the nested loop, then the program will output an infinite hold time.

Likewise, if the first fishbone within the fishbone valve fails at some time over the entire time domain (i.e. there exists a time t_j at which the actual spin frequency exceeds the burst frequency), then each of the subsequent fishbones will ultimately fail because the first fishbone has the largest burst frequency of all of the fishbones. In this case, the program will have a final value of "false" for the defined logic operator. If this logic operator is false then the program will add up the hold times of each of the individual fishbones. The *net hold time*, or the hold time of the entire capillary fishbone valve, is equal to the sum of the individual fishbone hold times. "Case 1" is the case for

which the individual fishbone hold times are all zero. "Case 3" is the case for which at least one of the individual fishbones has a hold time greater than zero.

The algorithm for this program is summarized in Appendix 6. The MATLAB code for this program is included in Appendix 7. Three sample outputs to this program are included in Appendix 8; each output corresponds to one of the three cases mentioned above. All of the input parameters are identical in each sample output except the actual spin frequency of the disk (*f*). Other input parameter values include 100 μm for the height of the channel, width of the channel, width of the fishbone, and distance between fishbones (*hc*, *wc*, *wf*, and *d*, respectively), the distance from the middle of the CD to the beginning of the fluid reservoir (*R1*) is 25,000 μm, the distance from the middle of the CD to the end of the flow front (*R2*) is 30,000 μm, the fluid density (ρ) is 1.0 g/cm^3, the air/liquid surface tension (γ) is 72.9 mN/m, the top view contact angle (θ) is 90 degrees, and the number of fishbones within the fishbone valve (*n*) is 5.

It should be noted that at this time no experimental work has been performed regarding the fishbone hold time. As a result, two kinetic models for $\Phi bot(t)$ and $\Phi top(t)$ have been arbitrarily chosen to clearly illustrate the concept of the capillary fishbone hold time. The time vector has been discretized into 6 values, ranging from 0 min to 5 min in increments 1 min. This small number was arbitrarily chosen to clearly illustrate the utility of the MATLAB program. In practice, the kinetic models would be determined experimentally and discretized into a larger number of elements.

6. RESULTS & DISCUSSION

6.1 Initial and Equilibrium Contact Angle Measurements

In order to predict the burst frequency of a fluid in a microchannel, the contact angle between the fluid and the solid must be known accurately. Empirical kinetic contact angle measurements were performed between the desired substrate and a 0.2 wt% BSA protein solution in a sealed chamber (experimental method 3.4). A 0.2 wt% BSA protein solution is used because it is representative of many biological fluids or protein solutions that are often used in ELISA. Three replicates were performed of each measurement.

Four PMMA substrates were tested: plasma treated and protein treated, plasma treated but not protein treated, protein treated but not plasma treated, and finally PMMA that was neither protein treated nor plasma treated. Protein treated industrial Scotch Tape was also tested. The channels of the PMMA microfluidic systems are currently closed with industrial Scotch tape which acts as the top channel surface.

The plasma treatment was performed using the method detailed in section 3.3. In order to protein treat a substrate, it was first cleaned with distilled water, soaked in a 1.0 wt% BSA (Bovine Serum Albumin) protein solution for 10 minutes, and then dried with a nitrogen hose. The BSA protein treatment simulates the protein blocking step that occurs in the ELISA process.

Empirically, it has been found that contact angle reaches equilibrium within 2 -3 minutes. As a result, the initial (0 min) and equilibrated (5 min) contact angles were measured for each of the substrates listed above. The results are summarized in Table 2.

Table 2: Initial and Equilibrium Contact Angles

Substrate Material	Plasma Treated	Protein Treated	Initial Contact Angle (0 min)	Equilibrium Contact Angle (5 min)	Δ
PMMA	N	N	73	68	5
PMMA	N	Y	74	42	32
PMMA	Y	Y	80	68	12
PMMA	Y	N	108	106	2
Scotch Tape	N	Y	106	105	1

Protein treatment decreases the initial contact angle and also increases the magnitude of the contact angle change between the initial and equilibrium contact angles. Due to protein treatment, the initial contact angle change was essentially negligible (~1 degree) between the plasma free PMMA samples while the initial contact angle change was very large (~28 degrees) between the plasma treated PMMA samples. Clearly, protein adsorption significantly disrupts the increased hydrophobic effect from the molecular layer of carbon hydrotriflouride. The magnitude of the decrease between the initial and equilibrium contact angles is greater for the protein treated samples versus the non-protein treated samples. This observation holds between both the plasma treated PMMA samples (~10 degrees) and plasma free PMMA samples (~27 degrees).

Plasma treatment increases the initial contact angle and also decreases the magnitude of the contact angle change between the initial and equilibrium contact angles. Due to plasma treatment, the initial contact angle change was very large (~35 degrees) between the non-protein treated PMMA samples while the initial contact angle change was much smaller (~6 degrees) between the protein treated PMMA samples. The magnitude of the decrease between the initial and equilibrium contact angles is less for the plasma treated samples than the plasma free samples. This decrease is greater between the protein treated PMMA samples (~20 degrees) than for the non-protein treated PMMA samples (~3 degrees).

Interestingly, the kinetic contact angle change between the 0.2 wt% BSA solution and the Scotch Tape was essentially negligible (~1 degree), indicating that very little protein adsorbed on the Scotch Tape surface.

The initial contact angle between the 0.2 wt% BSA solution and the plasma treated and protein treated PMMA is shown below in Figure 12.

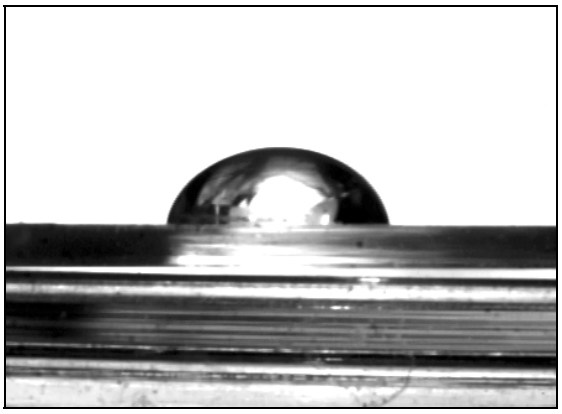

Figure 12: Contact Angle for Plasma Treated, Protein Treated PMMA

The equilibrium contact angle is shown below in Figure 13. Note the slight decrease in the contact angle between the liquid and the solid.

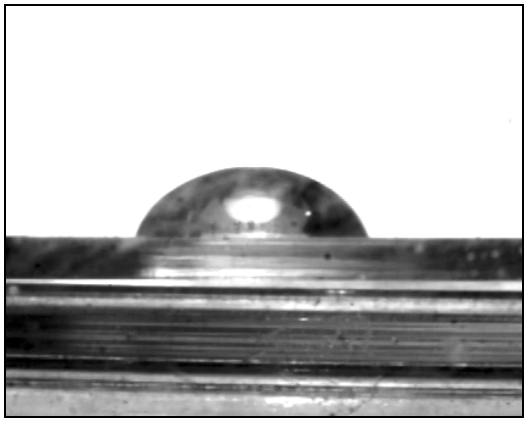

Figure 13: Equilibrium Contact Angle for Plasma Treated, Protein Treated PMMA

6.2 Empirical vs. Theoretical Burst Frequencies

The empirical burst frequencies of five microfluidic systems were tested and compared to the theoretical burst frequencies.

The PMMA microfluidic systems were made from PDMS molds (section 3.1) via the microembossing process (section 3.2). Each of these PMMA chips were plasma treated with a molecular layer of carbon hydrotriflouride (section 3.3). Each microfluidic system included a loading reservoir, a microchannel leading to a fishbone capillary valve, and a microchannel leading from the fishbone valve to a waste reservoir. These microfluidic systems were then cleaned, protein treated with BSA, and tested for empirical burst frequency measurements (experimental method 3.5).

Of the five microfluidic systems tested, the theoretical calculations correctly predicted three of the burst frequencies; i.e. the calculated burst frequency fell inside the empirically determined burst frequency range. This is a strong prediction considering the inherent error of the input parameters. The microfluidic chips were created by microembossing PMMA pellets with a PDMS mold. Thus, the geometry of the channels and fishbone valve possess an inherently moderate margin of error. Also, the burst frequency is very sensitive to the accuracy of the contact angle measurements. The model and theoretical calculations did a strong job at predicting these empirical results given the inherent error in the input parameters.

A summary of the theoretical vs. empirical results is shown below in Table 3.

Table 3: Summary of Empirical vs. Theoretical Burst Frequency Results

Valve #	Empirical Burst Freqency	Theoretical Burst Frequency	Inside Empirical Range?
1	761 - 791	787	Yes
2	705 - 736	650	No
3	478 - 511	498	Yes
4	541 - 572	501	No
5	574 - 606	603	Yes

The details for the theoretical vs. empirical burst frequency results for the first PMMA capillary valve tested is shown below in Table 4.

Table 4: Empirical vs. Theoretical Burst Frequency for 1st Capillary Fishbone Valve

PMMA Capillary Fishbone Valve #1	
Parameter	**Value**
Date	3/3/2006
Plasma Treated?	Yes
Protein Treated?	Yes
R1 (mm)	23.3
R2 (mm)	27.0
Width of Channel (µm)	200
Depth of Channel (µm)	100
Width of Fishbone (µm)	N/A
Distance b/w Fishbones (µm)	N/A
Theta (degrees)	80
Phi Top (degrees)	105
Phi Bottom (degrees)	68
Surface Tension (mN/m)	72.9
Fluid Density (g/cm^3)	1.0
Theoretical Burst Freq (RPM)	787
Empirical Burst Freq (RPM)	761 - 791
Inside Empirical Range?	**YES**

For this capillary fishbone valve, the theoretical burst frequency lies within the empirical burst frequency range. It should be noted that since the burst frequency of the first fishbone was tested, the width of the fishbone and the distance between fishbones are not relevant to this calculation. Any value for these two parameters can be input into the MATLAB program without influencing the end result. The contact angles are also of

note. A value of 80 degrees was assigned to θ, the top view contact angle. Since the polymer does not wet the side channel of the fishbone, the initial (0 min) contact angle between the 0.2 wt% BSA solution and the plasma treated - protein treated PMMA surface should be used. For the side view contact angle on the top surface, Φtop, a value of 105 degrees of was used. This value reflects the contact angle between the 0.2 wt% BSA solution and the protein-treated Scotch Tape after the surface has been wetted for at least five minutes. A value of 68 degrees was assigned to Φbot, the side view contact angle on the bottom surface. This value reflects the contact angle between the 0.2 wt% BSA solution and the plasma treated - protein treated PMMA after the surface has been wetted for at least five minutes.

The details of the theoretical vs. empirical results for each of the five fishbone capillary valves are included in Appendix 9.

Soon after the completion of this thesis, new microfluidic CD platforms with tighter manufacturing tolerances for the channel geometries will be available. These CD's were designed in AutoCAD with precise specifications. This design was sent to Ritek Corporation for high precision manufacturing. The empirical burst frequency measurements obtained from these CD's will be much more accurate, allowing the mathematical models and algorithms to be tested with further rigor. In addition, a larger sample size will be used in conjunction with these more accurate empirical measurements.

7. SUMMARY

Theory and mathematical modeling have been applied to quantitatively understand the behavior of the novel capillary fishbone valve. The general equation for the burst frequency of the *n*th fishbone within a capillary fishbone valve has been derived (equation 9). The fluid properties, the spin frequency of the microfluidic CD, and the geometry and location of the microchannels, reservoirs, and capillary fishbone valve will all affect the magnitude of the burst frequency (equation 10).

An algorithm has been developed to calculate the theoretical hold time of a capillary fishbone valve (section 5.2). This algorithm utilizes the derived burst frequency equations and kinetic models for the side view contact angle change with time.

Two user-friendly MATLAB computer programs have been written. One program calculates the burst frequency of the *n*th fishbone and the other program calculates the theoretical fishbone hold time in response to the key input parameters. These programs implement the models and algorithms in an easy-to-use form.

It should be noted that the theory, derivations, algorithms, and MATLAB computer programs described in this thesis are powerful design tools for the creation of the next generation microfluidic CD platform. In particular, it is now possible to maximize the theoretical burst frequency differences between sets of fishbone capillary valves. Also, it is now possible to estimate how many fishbones are needed within a capillary fishbone valve to yield the desired hold time. These calculations are in alignment with the original research objective, which was to increase the robustness and precision of the flow sequencing for the microfluidic CD platform.

BIBLIOGRAPHY

1. Madou, M. , Lee, L., Daunert, S., Lai., S., Shih, C., "Design and Fabrication of CD-like Microfluidic Platforms for Diagnostics: Microfluidic Functions," *Biomedical Microdevices*, **2001**, *3:3*, 245-254.

2. Lee, L., Madou, M., Koelling, K., Daunert, S., Lai, S., Koh, C., Juang, Y., Lu, Y., Yu, L., "Design and Fabrication of CD-like Microfluidic Platforms for Diagnostics: Polymer-Based Microfabrication," *Biomedical Devices*, **2001**, *3:4*, 339 – 351.

3. Lai, S., Wang, S., Luo, J., Lee, L., Yang, S., Madou, M., "Design of a Compact Disk-like Microfluidic Platform for Enzyme-Linked Immunosorbent Assay," *Anal. Chem.*, **2004**, *75*, 1832 – 1837.

4. Feng, Y., Zhou, Z., Ye, Xiongying, Y., Xiong, J., "Passive Valves Based on Hydrophobic Microfluidics," *Sensors and Actuators,* **2003**, *108*, 138 -143.

5. Kim, D., Lee, K., Kwon, T., Lee, S., "Microchannel Filling Flow Considering Surface Tension Effect," *J. Micromech. Microeng*., **2002**, *12*, 236 – 246.

6. Duffy, D., Gillis, H., Lin, J., Sheppard Jr., N., Kellog, G., "Microfabricated Centrifugal Microfluidic Systems: Characterization and Multiple Enzymatic Assays," *Anal. Chem.*, **1999**, *71*, 4669, 4678.

7. Yang, Y., Basu, S., Tomasko, D., Lee, L., Yang, S., "Fabrication of Well-Defined PLGA Scaffolds Using Novel Microembossing and Carbon Dioxide Bonding," *Biomaterials*, **2005**, *26*, 2585 – 2594.

8. Yang, Y., Zeng, C., Lee, L., "Three-Dimensional Assembly of Polymer Microstructures at Low Temperatures," *Advanced Materials*, **2004**, *16*, 560 – 564.

9. Madou, M. and Kellog, G., "The LabCD: A Centrifuge-Based Microfluidic Platform for Diagnostics," *SPIE Proceedings*, **1998**, *3259*, 80 – 92.

10. Squires, T. and Quake, S.., "Microfluidics: Fluid Physics at the Nanoliter Scale," *Rev. of Mod. Phys.*, **2005**, *77*, 977 – 1025.

11. Gravesen, P., Branebjerg, J., Jensen, O., "Microfluidics – A Review," *Micromech. Microeng.*, **1993**, *3*, 168 -182.

12. Darhuber, A., Valentino, J., Troian, S.; Wagner, S. "Thermocapillary Actuation of Droplets on Chemically Patterned Surfaces by Programmable Microheater Arrays." *J. Microelectromechanical Systems*, **2003**, 12, 873 – 879.

13. Nguyen, N., Truong, T., Wong, K., Ho, S., Lee, C., "Microvalves for Integration into Polymeric Microfluidic Devices," *J. Micromech. Microeng.*, **2004**, *14*, 69 – 75.

14. Jeon, N., Chiu, D., Wargo C., Wu, H., Choi, I., Anderson, J., Whiteside, G., "Microfluidics Section: Design and Fabrication of Integrated Passive Valves and Pumps for Flexible Polymer 3-Dimensional Microfluidic Systems," *Biomedical Microdevices*, **2002**, *4:2*, 117-121.

15. Schomburg, W., Fahrenberg, J., Maas, D., Rapp, R., "Active Valves and Pumps for Microfluidics," *J. Micromech. Microeng.*, **1993**, *3*, 216 – 218.

16. Cheng, J., Hsiung, L., "Electrowetting (EW)-Based Valve Combined with Hydrophilic Teflon Microfluidic Guidance in Controlling Continuous Fluid Flow," *Biomedical Microdevices*, **2004**, *6:4*, 341 – 347.

17. Suzuki, H., Yoneyama, R., "Integrate Microfluidic System with Electrochemically Activated On-Chip Pumps and Valves," Sensors and Actuators B, **2003**, *96*, 38 – 45.

18. Luo, Q., Mutlu, S., Gianchandani, Y., Svec, F., Fréchet, J., "Monolithic Valves for Microfluidic Chips Based on Thermoresponsive Polymer Gels," *Electrophoresis*, **2003**, *24*, 3694 – 3702.

APPENDIX

Appendix 1: *Derivation of the Net Capillary Pressure due to Surface Tension*

Rob Messinger

Derivation of ΔP_s, the capillary force per unit area due to surface tension.

i) Side View

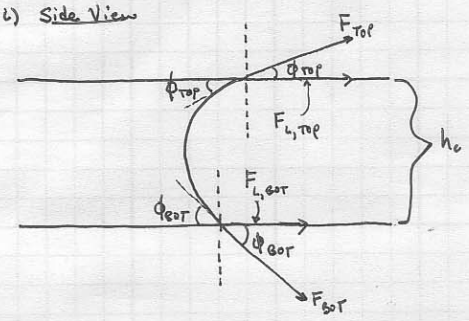

- $\cos\phi_{TOP} = \frac{F_{L,TOP}}{F_{TOP}}$

$F_{L,TOP} = F_{TOP}\cos\phi_{TOP}$

$\boxed{F_{L,TOP} = (\gamma \cdot w_c)\cos\phi_{TOP}}$

- $\cos\phi_{BOT} = \frac{F_{L,BOT}}{F_{BOT}}$

$F_{L,BOT} = F_{BOT}\cos\phi_{BOT}$

$\boxed{F_{L,BOT} = (\gamma \cdot w_c)\cos\phi_{BOT}}$

ii) Top View

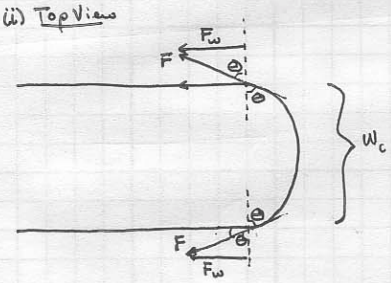

- Note $\theta_{TOP} = \theta_{BOT} = \theta$

$\sin\theta = \frac{F_w}{F}$

$F_w = F\sin\theta$

$\boxed{F_w = (\gamma \cdot h_c)\sin\theta}$

iii) Force Balance

$$\Delta P_s = 2\left[\frac{F_w}{A}\right] - \frac{F_{L,TOP}}{A} - \frac{F_{L,BOT}}{A}$$

since $A = w_c h_c$,

$$\Delta P_s = 2\left[\frac{(\gamma \cdot h_c)\sin\theta}{w_c h_c}\right] - \frac{(\gamma \cdot w_c)\cos\phi_{TOP}}{w_c h_c} - \frac{(\gamma \cdot w_c)\cos\phi_{BOT}}{w_c h_c}$$

$$\boxed{\Delta P_s = \gamma\left[\frac{2\cdot\sin\theta}{w_c} - \frac{\cos\phi_{TOP}}{h_c} - \frac{\cos\phi_{BOT}}{h_c}\right]}$$

22-141 50 SHEETS
22-142 100 SHEETS
22-144 200 SHEETS
AMPAD

Appendix 2: *Derivation of the Burst Frequency*

Rob Messinger

Derivation of f_b, the burst frequency.

- Set $\Delta P_c = \Delta P_s$ (centrifugal pressure = capillary pressure)
- Derivation of ΔP_c

$$\frac{dP_c}{dr} = \rho \omega^2 r$$

$$\int_{P_1}^{P_2} dP_c = \int_{R_1}^{R_2} \rho \omega^2 r \, dr$$

$$\Delta P_c = \frac{\rho \omega^2}{2} (R_2^2 - R_1^2)$$

$$\Delta P_c = \frac{\rho \omega^2}{2} (R_1 + R_2)(R_2 - R_1)$$

$$\boxed{\Delta P_c = \rho \omega^2 \Delta R \bar{R} \quad \text{where} \quad \begin{cases} \Delta R = R_2 - R_1 \\ \bar{R} = \frac{R_1 + R_2}{2} \end{cases}}$$

- Derivation of ΔP

As previously derived,

$$\boxed{\Delta P_s = \gamma \left[\frac{2 \cdot \sin\Theta}{w_c} - \frac{\cos\phi_{TOP}}{h_c} - \frac{\cos\phi_{BOT}}{h_c} \right]}$$

- Setting $\Delta P_c = \Delta P_s$,

$$\rho \omega_b^2 \Delta R \bar{R} = \gamma \left[\frac{2 \cdot \sin\Theta}{w_c} - \frac{\cos\phi_{TOP}}{h_c} - \frac{\cos\phi_{BOT}}{h_c} \right]$$

$$\omega_b^2 = \gamma \left[\frac{2 \cdot \sin\Theta}{w_c} - \frac{\cos\phi_{TOP}}{h_c} - \frac{\cos\phi_{BOT}}{h_c} \right] \Big/ (\rho \Delta R \bar{R})$$

since $\omega_b = 2\pi f_b$, $\omega_b^2 = 4\pi^2 f_b^2$

$$f_b^2 = \gamma \left[\frac{2 \cdot \sin\Theta}{w_c} - \frac{\cos\phi_{TOP}}{h_c} - \frac{\cos\phi_{BOT}}{h_c} \right] \Big/ (\rho \Delta R \bar{R} \cdot 4\pi^2)$$

$$\boxed{f_b = \left[\left(\frac{\gamma}{4\pi^2 \rho \Delta R \bar{R}} \right) \left(\frac{2 \cdot \sin\Theta}{w_c} - \frac{\cos\phi_{TOP}}{h_c} - \frac{\cos\phi_{BOT}}{h_c} \right) \right]^{1/2}}$$

22-141 50 SHEETS
22-142 100 SHEETS
22-144 200 SHEETS
AMPAD

Appendix 3: *Derivation o thef Burst Frequency of the* n*th Fishbone Valve*

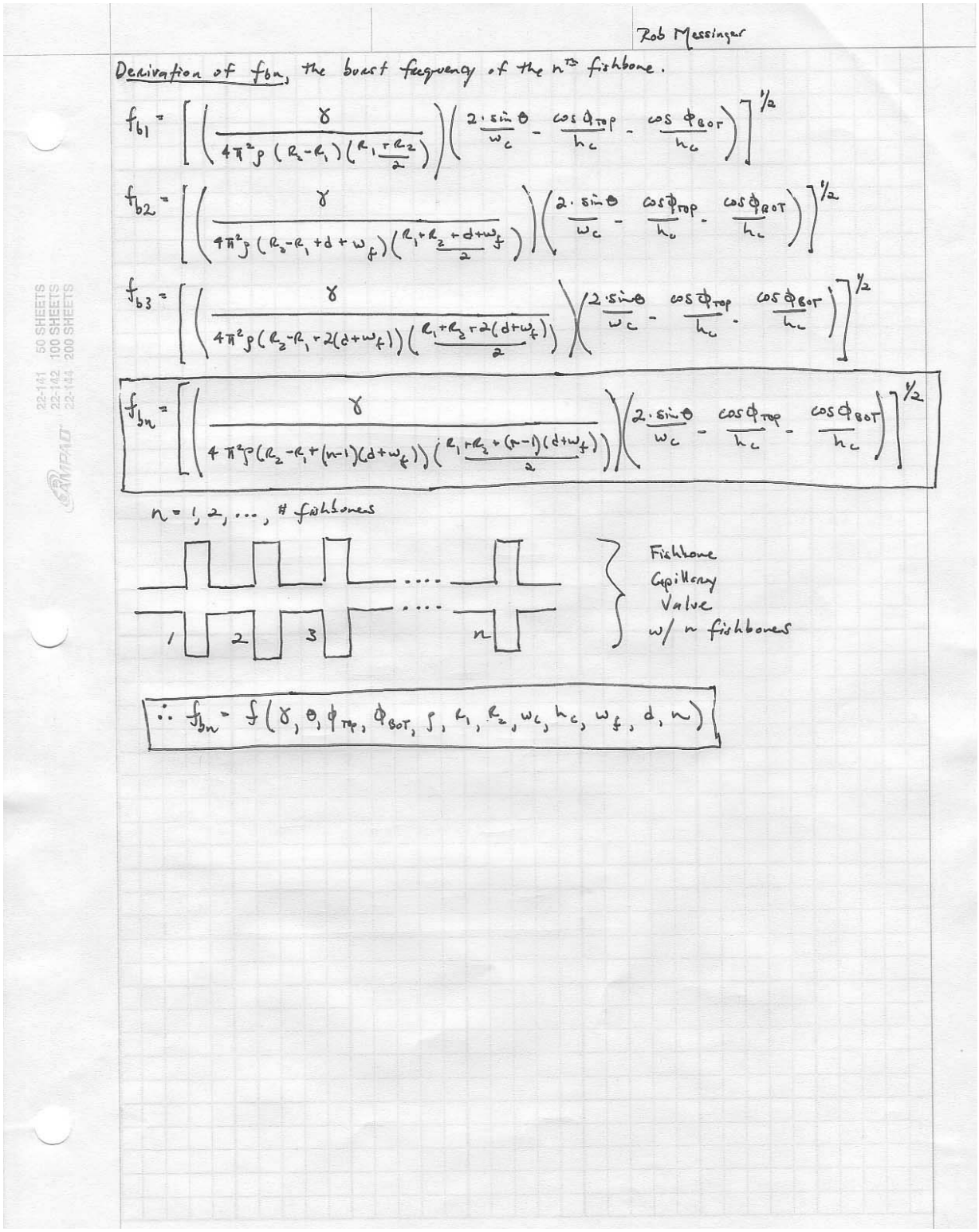

Appendix 4: *MATLAB Code; Calculates the Burst Frequency of an Array of Fishbones*

**********MATLAB Program Code**********

```
clear
clc

disp('This program calculates the burst frequency (rpm)')
disp('of the n fishbones in a specified fishbone valve.')
disp('     ')

%---------- USER INPUTS ----------&
disp('>>>>> CHANNEL & FISHBONE GEOMETRY <<<<<');
wc = input('Width of the channel (micrometers): ');
hc = input('Height of the channel (micrometers): ');
wf = input('Width of the fishbones (micrometers): ');
d = input('Distance between fishbones (micrometers): ');
n = input('Number of fishbones (integer): ');
disp('     ')

disp('>>>>> FLUID PROPERTIES <<<<<');
gam_mNm = input('Air/Liquid surface tension of the fluid (mN/m): ');
rho_gcm3 = input('Density of the fluid (g/cm^3): ');
theta_deg = input('Theta - contact angle top view (degrees): ');
phi_deg_top = input('Phi Top - contact angle side view (degrees): ');
phi_deg_bot = input('Phi Bottom - contact angle side view (degrees):
');
disp('     ')

disp('>>>>> FISHBONE VALVE POSITION <<<<<')
r1 = input('R1 (micrometers): ');
r2 = input('R2 (micrometers): ');
disp('     ')

%---------- Unit Converstions ----------%
gam = gam_mNm*10^3*(1/10^3);            %(g*m)/(s^2*m)
rho = rho_gcm3 * (100)^3/(1e6)^3;       %g/micrometers^3
theta = theta_deg*(2*pi)/360;           %radians
phi_top = phi_deg_top*(2*pi)/360;       %radians
phi_bot = phi_deg_bot*(2*pi)/360;       %radians

%---------- Burst Frequency Calculations ----------&
for i = 1:1:n
    a = (4*pi^2*rho)/gam;
    b = (2*sin(theta)/wc - cos(phi_top)/hc - cos(phi_bot)/hc);
    r_delta = r2+(i-1)*(d+wf)-r1;
    r_bar = (r1+r2+(i-1)*(d+wf))/2;
    fb(i) = sqrt(b/(a*r_delta*r_bar))*60;  %rpm
end

disp('fb(n) = ')
disp(fb')
```

Appendix 5: *MATLAB Ouput; Calculates the Burst Frequency of an Array of Fishbones*

```
**********MATLAB Program Output**********
This program calculates the burst frequency (rpm)
of the n fishbones in a specified fishbone valve.

>>>>> CHANNEL & FISHBONE GEOMETRY <<<<<
Width of the channel (micrometers): 100
Height of the channel (micrometers): 100
Width of the fishbones (micrometers): 100
Distance between fishbones (micrometers): 100
Number of fishbones (integer): 5

>>>>> FLUID PROPERTIES <<<<<
Air/Liquid surface tension of the fluid (mN/m): 72.9
Density of the fluid (g/cm^3): 1
Theta - contact angle top view (degrees): 90
Phi Top - contact angle side view (degrees): 90
Phi Bottom - contact angle side view (degrees): 80

>>>>> FISHBONE VALVE POSITION <<<<<
R1 (micrometers): 25000
R2 (micrometers): 30000

fb(n) =
  939.6714
  919.7529
  900.9291
  883.1022
  866.1862
```

Appendix 6: *Summary of Fishbone Hold Time Algorithm*

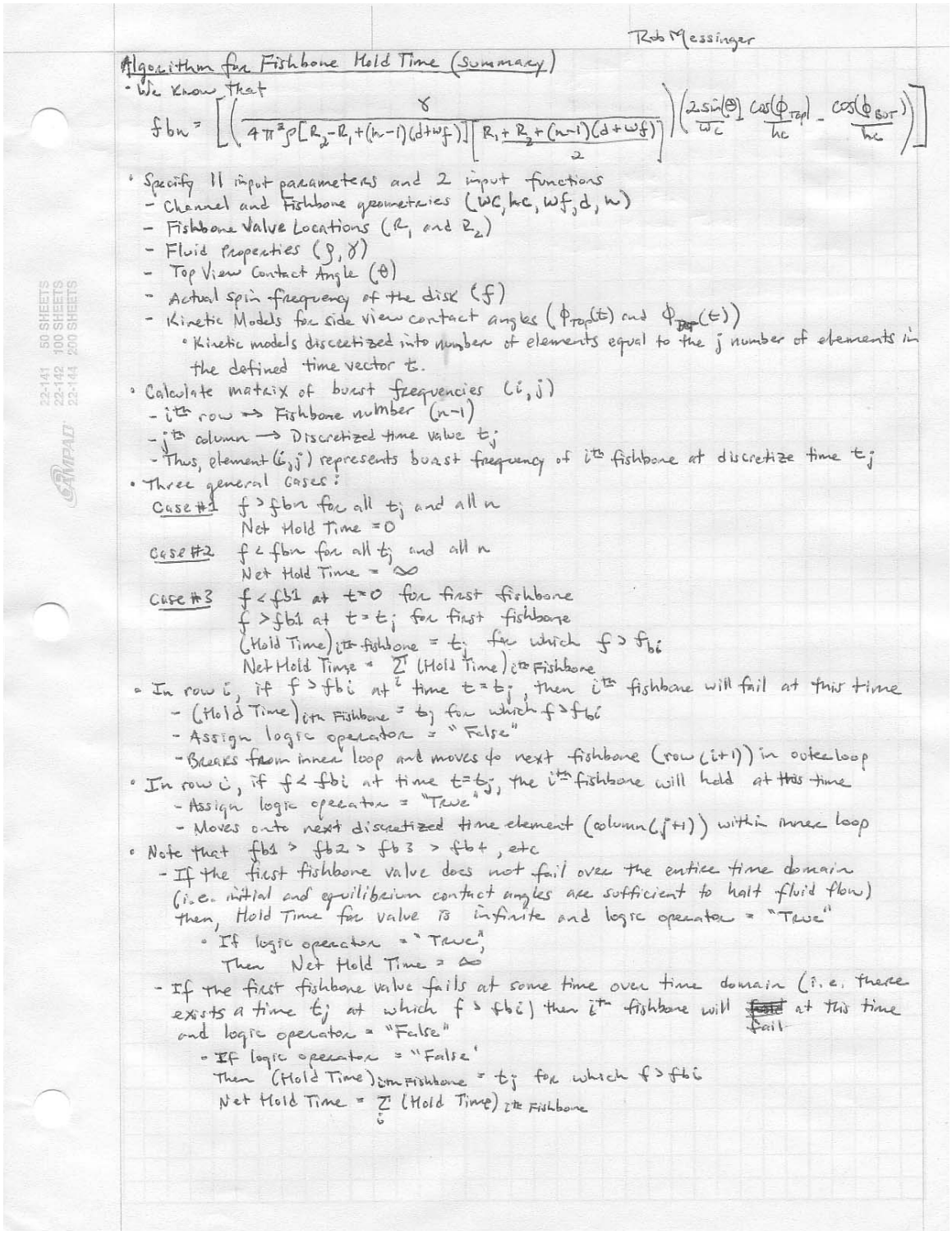

Rob Messinger

Algorithm for Fishbone Hold Time (Summary)

- We know that

$$f_{bn} = \left[\left(\frac{\gamma}{4\pi^2\rho\left[R_2-R_1+(n-1)(d+w_f)\right]\left[R_1+\frac{R_2+(n-1)(d+w_f)}{2}\right]}\right)\left(\frac{2\sin(\theta)}{w_c}\left[\frac{\cos(\phi_{Top})}{h_c}-\frac{\cos(\phi_{BOT})}{h_c}\right)\right)\right]$$

- Specify 11 input parameters and 2 input functions
  - Channel and Fishbone geometries (w_c, h_c, w_f, d, n)
  - Fishbone Valve Locations (R_1 and R_2)
  - Fluid Properties (ρ, γ)
  - Top View Contact Angle (θ)
  - Actual spin frequency of the disk (f)
  - Kinetic Models for side view contact angles ($\phi_{Top}(t)$ and $\phi_{Bot}(t)$)
    - Kinetic models discretized into number of elements equal to the j number of elements in the defined time vector t.
- Calculate matrix of burst frequencies (i, j)
  - i^{th} row → Fishbone number $(n-1)$
  - j^{th} column → Discretized time value t_j
  - Thus, element (i, j) represents burst frequency of i^{th} fishbone at discretize time t_j
- Three general cases:

  Case #1: $f > f_{bn}$ for all t_j and all n
  Net Hold Time = 0

  Case #2: $f < f_{bn}$ for all t_j and all n
  Net Hold Time = ∞

  Case #3: $f < f_{b1}$ at $t=0$ for first fishbone
  $f > f_{b1}$ at $t = t_j$ for first fishbone
  $(\text{Hold Time})_{i^{th}\text{ fishbone}} = t_j$ for which $f > f_{bi}$
  Net Hold Time = $\sum_{i}^{n} (\text{Hold Time})_{i^{th}\text{ Fishbone}}$

- In row i, if $f > f_{bi}$ at i^{th} time $t = t_j$, then i^{th} fishbone will fail at this time
  - $(\text{Hold Time})_{i^{th}\text{ Fishbone}} = t_j$ for which $f > f_{bi}$
  - Assign logic operator = "False"
  - Breaks from inner loop and moves to next fishbone (row $(i+1)$) in outer loop
- In row i, if $f < f_{bi}$ at time $t = t_j$, the i^{th} fishbone will hold at this time
  - Assign logic operator = "True"
  - Moves onto next discretized time element (column $(j+1)$) within inner loop
- Note that $f_{b1} > f_{b2} > f_{b3} > f_{b4}$, etc
  - If the first fishbone valve does not fail over the entire time domain (i.e. initial and equilibrium contact angles are sufficient to halt fluid flow) then, Hold Time for valve is infinite and logic operator = "True"
    - If logic operator = "True",
      Then Net Hold Time = ∞
  - If the first fishbone valve fails at some time over time domain (i.e. there exists a time t_j at which $f > f_{bi}$) then i^{th} fishbone will ~~fail~~ fail at this time and logic operator = "False"
    - If logic operator = "False"
      Then $(\text{Hold Time})_{i^{th}\text{ Fishbone}} = t_j$ for which $f > f_{bi}$
      Net Hold Time = $\sum_{i}^{n} (\text{Hold Time})_{i^{th}\text{ Fishbone}}$

Appendix 7: *MATLAB Code; Calculates the Theoretical Hold Time of Fishbone Valve*

**********MATLAB Program Code**********

```
clear
clc

disp('     ')
disp('This program calculates the theoretical hold time')
disp('(min) of a capillary fishbone valve with n fishbones.')
disp('     ')

%-------------------- USER INPUTS --------------------&
disp('>>>>> CHANNEL & FISHBONE GEOMETRY <<<<<');
wc = input('Width of the channel (micrometers): ');
hc = input('Height of the channel (micrometers): ');
wf = input('Width of the fishbones (micrometers): ');
d = input('Distance between fishbones (micrometers): ');
n = input('Number of fishbones (integer): ');
disp('     ')

disp('>>>>> FLUID PROPERTIES <<<<<');
gam_mNm = input('Air/Liquid surface tension of the fluid (mN/m): ');
rho_gcm3 = input('Density of the fluid (g/cm^3): ');
disp('     ')

disp('>>>>> FISHBONE VALVE POSITION <<<<<')
r1 = input('R1 (micrometers): ');
r2 = input('R2 (micrometers): ');
disp('     ')

disp('>>>>> SETTINGS <<<<<')
f = input('Spin Frequency (RPM): ');
disp('     ')

disp('>>>>> PREFERENCES <<<<<')
option = input('Would you like to display the burst frequencies of each
of the individual fishbones? (yes = 1, no = 0)');
disp('     ')

disp('>>>>> KINETIC MODEL <<<<<')
disp('*****Accurate kinetic model to be determined*****')
disp('     ')
t = [0:1:5];                              %min
phi_top_deg = exp(-t./5).*10 + 80;        %kinetic model (t)
phi_bot_deg = exp(-t./5).*10 + 50;        %kinetic model (t)
theta_deg = 90;                           %surface not wetted

%-------------------- Unit Converstions --------------------%
gam = gam_mNm*10^3*(1/10^3);              %(g*m)/(s^2*m)
rho = rho_gcm3 * (100)^3/(1e6)^3;         %g/micrometers^3
theta = theta_deg*(2*pi)/360;             %radians
phi_top = phi_top_deg.*(2*pi)/360;        %radians
phi_bot = phi_bot_deg.*(2*pi)/360;        %radians
```

```
%--------------- Burst Frequency Matrix ---------------&
for i = 1:1:n
    for j = 1:1:numel(t)
        a = (4*pi^2*rho)/gam;
        b = (2*sin(theta)/wc - cos(phi_top(j))/hc -
cos(phi_bot(j))/hc);
        r_delta = r2+(i-1)*(d+wf)-r1;
        r_bar = (r1+r2+(i-1)*(d+wf))/2;
        fb(i,j) = sqrt(b./(a.*r_delta.*r_bar)).*60;  %rpm
    end
end

%--------------- Holding Time Calculations -----------------&
for i = 1:1:n
    for j = 1:1:numel(t)
        if fb(i,j) < f
           hold(i) = t(j);
           logic_loop(i) = 0;
           break
        else
           logic_loop(i) = 1;
        end
    end
end

logic = logic_loop(1);

if logic == false
    hold_time = sum(hold);
    disp('The hold time (min) of each fishbone in the fishbone valve
is: ')
    hold
    disp('     ')
    disp('The net hold time (min) of the entire fishbone valve is: ')
    hold_time
    disp('     ')
elseif logic == true
    hold_time = inf;
    disp('*****THE VALVE WILL NOT FAIL UNDER THESE CONDITIONS******')
    disp('     ')
    hold_time
    disp('     ')
end

%--------------- Preferences -----------------&
if option == 1
    disp('The kinetic burst frequency of each individual fishbone is:')
    fb
end
```

Appendix 8: *MATLAB Output; Calculates the Theoretical Hold Time of Fishbone Valve*

**********MATLAB Program Output (CASE 1)**********
This program calculates the theoretical hold time
(min) of a capillary fishbone valve with n fishbones.

>>>>> CHANNEL & FISHBONE GEOMETRY <<<<<
Width of the channel (micrometers): 100
Height of the channel (micrometers): 100
Width of the fishbones (micrometers): 100
Distance between fishbones (micrometers): 100
Number of fishbones (integer): 5

>>>>> FLUID PROPERTIES <<<<<
Air/Liquid surface tension of the fluid (mN/m): 72.9
Density of the fluid (g/cm^3): 1

>>>>> FISHBONE VALVE POSITION <<<<<
R1 (micrometers): 25000
R2 (micrometers): 30000

>>>>> SETTINGS <<<<<
Spin Frequency (RPM): 1000

>>>>> PREFERENCES <<<<<
Would you like to display the burst frequencies of each of the individual fishbones? (yes = 1, no = 0)1

>>>>> KINETIC MODEL <<<<<
*****Accurate kinetic model to be determined*****

The hold time (min) of each fishbone in the fishbone valve is:

hold =

    0   0   0   0   0

The net hold time (min) of the entire fishbone valve is:

hold_time =

    0

The kinetic burst frequency of each individual fishbone is:

fb =

```
  851.5878  834.7367  820.8045  809.3092  799.8398  792.0488
  833.5364  817.0425  803.4056  792.1540  782.8853  775.2595
  816.4771  800.3208  786.9630  775.9417  766.8627  759.3929
  800.3213  784.4846  771.3912  760.5879  751.6886  744.3666
  784.9910  769.4577  756.6150  746.0188  737.2898  730.1081

**********MATLAB Program Output (CASE 2)**********
This program calculates the theoretical hold time
(min) of a capillary fishbone valve with n fishbones.

>>>>> CHANNEL & FISHBONE GEOMETRY <<<<<
Width of the channel (micrometers): 100
Height of the channel (micrometers): 100
Width of the fishbones (micrometers): 100
Distance between fishbones (micrometers): 100
Number of fishbones (integer): 5

>>>>> FLUID PROPERTIES <<<<<
Air/Liquid surface tension of the fluid (mN/m): 72.9
Density of the fluid (g/cm^3): 1

>>>>> FISHBONE VALVE POSITION <<<<<
R1 (micrometers): 25000
R2 (micrometers): 30000

>>>>> SETTINGS <<<<<
Spin Frequency (RPM): 800

>>>>> PREFERENCES <<<<<
Would you like to display the burst frequencies of each of the individual fishbones? (yes
= 1, no = 0)1

>>>>> KINETIC MODEL <<<<<
*****Accurate kinetic model to be determined*****

The hold time (min) of each fishbone in the fishbone valve is:

hold =

    4     3     2     1     0

The net hold time (min) of the entire fishbone valve is:

hold_time =
```

10

The kinetic burst frequency of each individual fishbone is:

fb =

851.5878	834.7367	820.8045	809.3092	799.8398	792.0488
833.5364	817.0425	803.4056	792.1540	782.8853	775.2595
816.4771	800.3208	786.9630	775.9417	766.8627	759.3929
800.3213	784.4846	771.3912	760.5879	751.6886	744.3666
784.9910	769.4577	756.6150	746.0188	737.2898	730.1081

**********MATLAB Program Output (CASE 3)**********
This program calculates the theoretical hold time
(min) of a capillary fishbone valve with n fishbones.

>>>>> CHANNEL & FISHBONE GEOMETRY <<<<<
Width of the channel (micrometers): 100
Height of the channel (micrometers): 100
Width of the fishbones (micrometers): 100
Distance between fishbones (micrometers): 100
Number of fishbones (integer): 5

>>>>> FLUID PROPERTIES <<<<<
Air/Liquid surface tension of the fluid (mN/m): 72.9
Density of the fluid (g/cm^3): 1

>>>>> FISHBONE VALVE POSITION <<<<<
R1 (micrometers): 25000
R2 (micrometers): 30000

>>>>> SETTINGS <<<<<
Spin Frequency (RPM): 600

>>>>> PREFERENCES <<<<<
Would you like to display the burst frequencies of each of the individual fishbones? (yes = 1, no = 0)1

>>>>> KINETIC MODEL <<<<<
*****Accurate kinetic model to be determined*****

*****THE VALVE WILL NOT FAIL UNDER THESE CONDITIONS******

hold_time =

Inf

The kinetic burst frequency of each individual fishbone is:

fb =

851.5878	834.7367	820.8045	809.3092	799.8398	792.0488
833.5364	817.0425	803.4056	792.1540	782.8853	775.2595
816.4771	800.3208	786.9630	775.9417	766.8627	759.3929
800.3213	784.4846	771.3912	760.5879	751.6886	744.3666
784.9910	769.4577	756.6150	746.0188	737.2898	730.1081

Appendix 9: *Details of Theoretical vs. Empirical Burst Frequency Measurements*

PMMA Capillary Fishbone Valve #1	
Parameter	**Value**
Date	3/3/2006
Plasma Treated?	Yes
Protein Treated?	Yes
R1 (mm)	23.3
R2 (mm)	27.0
Width of Channel (μm)	200
Depth of Channel (μm)	100
Width of Fishbone (μm)	N/A
Distance b/w Fishbones (μm)	N/A
Theta (degrees)	80
Phi Top (degrees)	105
Phi Bottom (degrees)	68
Surface Tension (mN/m)	72.9
Fluid Density (g/cm^3)	1.0
Theoretical Burst Freq (RPM)	787
Empirical Burst Freq (RPM)	761 - 791
Inside Empirical Range?	**YES**

PMMA Capillary Fishbone Valve #2	
Parameter	**Value**
Date	3/7/2006
Plasma Treated?	Yes
Protein Treated?	Yes
R1 (mm)	21.6
R2 (mm)	27.2
Width of Channel (μm)	200
Depth of Channel (μm)	100
Width of Fishbone (μm)	N/A
Distance b/w Fishbones (μm)	N/A
Theta (degrees)	80
Phi Top (degrees)	105
Phi Bottom (degrees)	68
Surface Tension (mN/m)	72.9
Fluid Density (g/cm^3)	1.0
Theoretical Burst Freq (RPM)	650
Empirical Burst Freq (RPM)	705 - 736
Inside Empirical Range?	**NO**

PMMA Capillary Fishbone Valve #3	
Parameter	**Value**
Date	3/7/2006
Plasma Treated?	Yes
Protein Treated?	Yes
R1 (mm)	32.5
R2 (mm)	39.0
Width of Channel (µm)	200
Depth of Channel (µm)	100
Width of Fishbone (µm)	N/A
Distance b/w Fishbones (µm)	N/A
Theta (degrees)	80
Phi Top (degrees)	105
Phi Bottom (degrees)	68
Surface Tension (mN/m)	72.9
Fluid Density (g/cm^3)	1.0
Theoretical Burst Freq (RPM)	498
Empirical Burst Freq (RPM)	478 - 511
Inside Empirical Range?	**YES**

PMMA Capillary Fishbone Valve #4	
Parameter	**Value**
Date	3/7/2006
Plasma Treated?	Yes
Protein Treated?	Yes
R1 (mm)	39.0
R2 (mm)	44.5
Width of Channel (µm)	200
Depth of Channel (µm)	100
Width of Fishbone (µm)	N/A
Distance b/w Fishbones (µm)	N/A
Theta (degrees)	80
Phi Top (degrees)	105
Phi Bottom (degrees)	68
Surface Tension (mN/m)	72.9
Fluid Density (g/cm^3)	1.0
Theoretical Burst Freq (RPM)	501
Empirical Burst Freq (RPM)	541 - 572
Inside Empirical Range?	**NO**

PMMA Capillary Fishbone Valve #5	
Parameter	**Value**
Date	3/7/2006
Plasma Treated?	Yes
Protein Treated?	Yes
R1 (mm)	25.5
R2 (mm)	31.1
Width of Channel (μm)	200
Depth of Channel (μm)	100
Width of Fishbone (μm)	N/A
Distance b/w Fishbones (μm)	N/A
Theta (degrees)	80
Phi Top (degrees)	105
Phi Bottom (degrees)	68
Surface Tension (mN/m)	72.9
Fluid Density (g/cm^3)	1.0
Theoretical Burst Freq (RPM)	603
Empirical Burst Freq (RPM)	574 - 606
Inside Empirical Range?	**YES**